www.shd.org.yu

Journal of the Serbian Chemical Society
eVersion
electronic

JSCS@tmf.bg.ac.yu • www.shd.org.yu/JSCS

J. Serb. Chem. Soc. 73 (4) 479–486 (2008)
JSCS–3729

UDC 546.654.027*123+544.773.42:
:542.913.004.12:621.315
Original scientific paper

Synthesis and characterization of Ln-123 superconductors

ARTURAS ZALGA[1], REMIGIJUS JUSKENAS[2], ALGIRDAS SELSKIS[2],
DARIUS JASAITIS[1] and AIVARAS KAREIVA[1]*

[1]*Faculty of Chemistry, Vilnius University, Naugarduko 24, LT-03225 Vilnius and* [2]*Institute of Chemistry, A. Gostauto 9, LT-01108 Vilnius, Lithuania*

(Received 10 January, revised 12 November 2007)

Abstract: A sol–gel method was applied to prepare precursors for $NdBa_2Cu_3O_{7-x}$ (Nd-123) and $SmBa_2Cu_3O_{7-x}$ (Sm-123) superconducting compounds. The sintered products were examined by X-ray diffraction analysis (XRD) and scanning electron microscopy (SEM). The powders sintered at 950 and 1000 °C showed the formation of monophasic Nd-123 and Sm-123 superconductors. The formation of Nd-123 and Sm-123 phases from the sol-gel derived precursors at higher temperatures (1050 and 1100 °C), however, did not proceed due to the melting process. The correlation between the T_C for different lanthanides (Ln – Ho, Nd and Sm) in the Ln-123 compound and orthorhombicity and oxygen stoichiometry were also estimated.

Keywords: 123 superconductors; substitution effects; lanthanides; sol–gel synthesis.

INTRODUCTION

Practical application of high-temperature superconductors requires long length and complex shapes of the textured ceramic materials.[1,2] An important step in the fabrication of such superconducting architectures is the development of joining technologies between individual superconducting components.[3] Two melt-textured $YBa_2Cu_3O_{7-x}$ superconducting blocks can be successfully welded with $LnBa_2Cu_3O_{7-x}$ (Ln – rare earth element) solders.[4] For almost all practical applications – large and small scale – the superconducting ceramics must carry sufficiently large electrical currents, typically > 10^6 A cm^{-2} and operate in strong magnetic fields. It is a consequence of poor reproducibility of the critical transport current density in bulk ceramic high-temperature superconductors that enormous interest in the development of new synthetic methods for their preparation continues.

The critical transport current density in bulk ceramic high-temperature super–conductors, such as $LnBa_2Cu_3O_{7-x}$, is highly dependent on the microstructure.[5–8]

---

* Corresponding author. E-mail: aivaras.kareiva@chf.vu.lt

doi: 10.2298/JSC0804479Z

For most of the multimetallic oxides, an unusual combination of physical and chemical properties depends largely on the compositional homogeneity, phase purity, surface morphology and microstructure. These features crucial for the preparation of electronic, optic and catalytic materials are dependent on the method of synthesis.[2]

Obviously the variation of homogeneity region, as well as the structural and superconducting properties in $LnBa_2Cu_3O_{7-x}$ superconductors should also be very dependent on the employed preparation technique.[6,9] Recently, a simple *chimie douce* synthetic approach was developed to obtain a high-purity crystalline $HoBa_2Cu_3O_{7-x}$ superconducting phase by heat treatment of mixed-metal gels at different temperatures.[10] The powders sintered at 950 and 1000 °C showed the formation of monophasic Ho-123 superconductors. The formation of the Ho-123 phase from sol–gel derived precursors at higher temperatures (1050 and 1100 °C) was, however, strongly controlled by the peritectic reaction Ho-211 + + L $\rightleftarrows$ Ho-123. Also, the effect of holmium substitution on the structural and surface morphological properties of Y-123 superconductors synthesized by sol–gel technique was studied.

Clearly, the difference in the ionic radius of the Ln ion has an effect on the superconductivity of Ln-123.[9,11,12] In the present study, the Ho^{3+} ion (r = 1.07 Å) in Ho-123 was replaced by the larger Nd^{3+} (r = 1.16 Å) and Sm^{3+} ion (r = 1.32 Å) and the effect of the lanthanide substitution on the oxygen stoichiometry, superconducting properties and the orthorhombicity of the unit cell of the resulting Ln-123 (Ln – Ho, Nd, Sm) was studied.

EXPERIMENTAL

$LnBa_2Cu_3O_{7-x}$ (Ln – Nd, Sm) were synthesized by a two-step method in which a precursor was first synthesized using the sol–gel technique and then calcined at different temperatures. In the sol–gel process, stoichiometric amounts of Nd_2O_3, Sm_2O_3, $Cu(CH_3COO)_2{\cdot}H_2O$ and $Ba(CH_3COO)_2$ (all of analytical grade) were used as the starting compounds. The Nd_2O_3 or Sm_2O_3 was first dissolved in 0.20 M acetic acid at 55–60 °C. Next, $Ba(CH_3COO)_2$ and $Cu(CH_3COO)_2{\cdot}H_2O$, dissolved in a small amount of distilled water, were added with intermediate stirring during several hours at the same temperature. A solution of tartaric acid in water was added to adjust the pH to 5.6, thus preventing crystallization of copper acetate during gelation. The obtained solutions were concentrated during about 8 hours at 60–65 °C in an open beaker. Under continuous stirring, the transparent blue Nd–Ba–Cu–O and Sm–Ba–Cu–O precursor gels formed. After further drying in an oven at 80 °C, fine-grained blue powders were obtained. The precursor powders were placed in an alumina crucible and calcined for 10 h at 850 °C in an oxygen atmosphere, reground in an agate mortar and pelletized. The pellets were again placed in an alumina crucible and, starting from room temperature, annealed in an ordinary tube furnace for 5 h at different temperatures (950, 1000, 1050 and 1100 °C). The heating and cooling rate was 5 °C min^{-1}. At the end of the growth experiment, the crystals were cooled in the furnace to 200 °C and crucible was raised from the furnace. Finally, the crystals obtained at different temperatures were annealed for 10 h at 500 °C in oxygen to be converted into the orthorhombic superconducting form.[13]

The X-ray powder diffraction (XRD) studies were performed on a STOE diffractometer operating with CuKα_1 radiation. The lattice parameters of the synthesized samples were obtained from the diffraction spectra by fitting the peaks of the identified reflections using a least-squares procedure.[6,14,15] A scanning electron microscope (SEM) JXA-50A JEOL was used to study the morphology and microstructure of the ceramic samples. T_C values of the superconducting compounds were obtained from magnetic susceptibility measurements performed in gelatine capsules with a SQUID magnetometer (Quantum Design, MPMS) in the temperature region between 5 and 120 K. The oxygen content in the superconducting samples was determined by the well-known iodometric titration method.[16-18]

RESULTS AND DISCUSSION

As was already previously reported, the sintering of a Ho–Ba–Cu–O precursor gel at 950 or 1000 °C produced a fully crystalline single-phase $HoBa_2Cu_3O_{7-x}$ superconducting oxide.[10] Further heating to 1050–1100 °C, however, resulted in XRD patterns indicating the definite presence of different phases. The following Equations describe the equilibria in the investigated system at 1050 and 1100 °C, respectively:

$$2HoBa_2Cu_3O_{7-x} \rightleftarrows Ho_2BaCuO_5 + 1.5Ba_2Cu_3O_{5+x} + 0.5CuO + (0.5 - 1{,}75x)O_2 \quad (1)$$

$$2HoBa_2Cu_3O_{7-x} \rightleftarrows Ho_2BaCuO_5 + 3BaCuO_2 + 2CuO + (0.5 - x)O_2 \quad (2)$$

The Nd–Ba–Cu–O and Sm–Ba–Cu–O gel powders sintered at 950 and 1000 °C also showed the formation of single phase Nd-123 and Sm-123 superconductors, respectively. However, contrary to the case of holmium, the heating of neodymium and samarium starting materials at higher temperatures (1050 and 1100 °C) gave fully melted synthesis products, the compositions of which were not analyzed.

The textural properties of the calcined Nd–Ba–Cu–O precursor gels at different temperatures (950, 1000, 1050, and 1100 °C) are shown in Fig. 1.

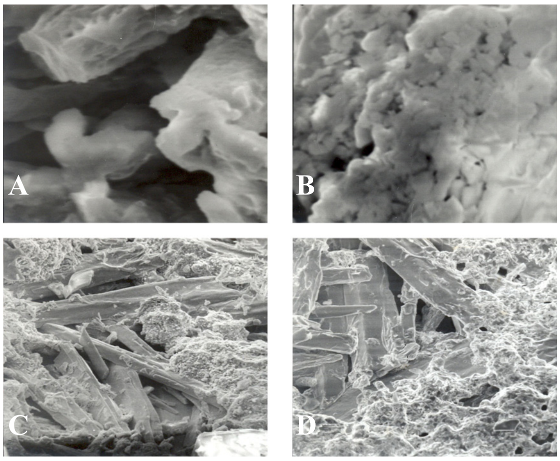

Fig. 1. Scanning electron micrographs of the Nd–Ba–Cu–O precursor gels annealed at 950 °C (C), 1000 °C (D), 1050 °C (A) and 1100 °C (B). Magnification 170×.

The microstructure of the $NdBa_2Cu_3O_{7-x}$ ceramic sample obtained at 950 °C was composed of a number of elongated grains. The SEM micrograph of the powders calcined at 1000 °C shows that the individual particles seem to be also stick-like crystals. A progressive change in the morphology was evident with increasing calcination temperature. The micrograph of the specimen sintered at 1050 °C shows a lack of grain growth and an undeveloped microstructure due to the partial melting of the specimen at this temperature. The microstructure of the sample obtained at 1100 °C consisted of a clustered matrix, which is typical for a melted ceramic product. The surface features of the Sm–Ba–Cu–O precursor gels calcined at the same temperatures (950, 1000, 1050, and 1100 °C) are shown in Fig. 2.

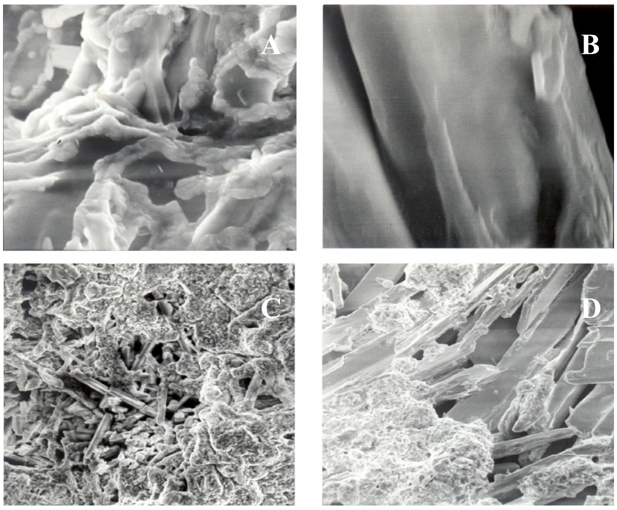

Fig. 2. Scanning electron micrographs of the Sm–Ba–Cu–O precursor gels annealed at 1050 °C (A), 1100 °C (B), 950 °C (C) and 1000 °C (D). Magnification 170×.

Evidently, the ceramic samples obtained by sintering the Sm–Ba–Cu–O precursor gels at 950, 1000, 1050 and 1100 °C had a similar microstructure to those of the Nd-based samples.

The lattice parameters and orthorhombicity of the $LnBa_2Cu_3O_{7-x}$ superconducting cuprates synthesized at 950 °C and 1000 °C are given in Table I.

TABLE I. Lattice parameters and orthorhombicity, $2(b-a)/(a+b)$, of $LnBa_2Cu_3O_{7-x}$

Sample	Temperature °C	a / Å	b / Å	c / Å	V / Å^3	Orthorhombicity
$HoBa_2Cu_3O_{7-x}$	950	3.855	3.907	11.684	176.0	0.0133
	1000	3.857	3.907	11.680	176.0	0.0129
$NdBa_2Cu_3O_{7-x}$	950	3.868	3.914	11.749	177.9	0.0117
	1000	3.867	3.915	11.753	177.9	0.0122
$SmBa_2Cu_3O_{7-x}$	950	3.889	3.924	11.763	179.5	0.0090
	1000	3.890	3.926	11.761	179.6	0.0092

As can be seen, all the samples crystallized into the orthorhombic Ln-123 phase, indicating that the systems did not tend towards tetragonality on changing the lanthanide ion. Moreover, the lattice parameters and orthorhombicity obtained for the samples containing the same lanthanide ion but synthesized at different temperatures were very similar. Figures 3 and 4 show that the mean values of all lattice parameters of $LnBa_2Cu_3O_{7-x}$ oxides synthesized at 950 and 1000 °C slightly increased with increasing ionic radius of the rare earth element.

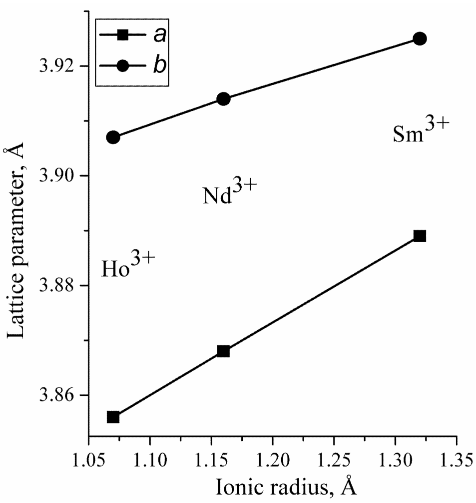

Fig. 3. Lattice parameters (a and b) as a function of ionic radius.

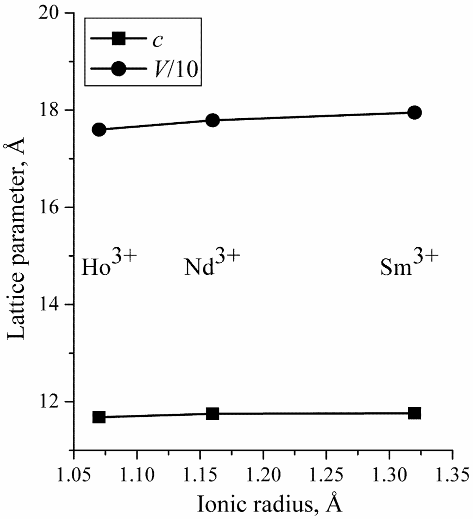

Fig. 4. Lattice parameters (c and V) as a function of ionic radius.

Figure 5 shows that the orthorhombicity decreased almost linearly with increasing ionic radius of the Ln^{3+} ion.

The orthorhombicity, $2(b - a)/(a + b)$, is a measure of the length difference between the b- and a-axis, which is related to the occupancy of the oxygen atom sites at O(4) and O(5) in the basal plane, respectively.[9] Therefore, the oxygen content in the superconducting $LnBa_2Cu_3O_{7-x}$ samples was also determined. The results of the determination of the oxygen stoichiometery, x, were used for the calculation of the hole concentration (n_h) in the Cu–O chains. According to the literature,[6] the chain hole concentration is $(7 - x) - 6.5$. The oxygen stoichiometry, hole concentration and T_C values of the $LnBa_2Cu_3O_{7-x}$ superconductors are listed in Table II.

As can be seen, the specimens found to be superconducting had a T_C (onset) of 89, 91 and 93.5 K for $HoBa_2Cu_3O_{7-x}$, $NdBa_2Cu_3O_{7-x}$ and $SmBa_2Cu_3O_{7-x}$, respectively. In addition, it is evident that the obtained parameters (x, n_h, T_C (onset), T_C (zero)) did not depend on the preparation temperature.

Figure 6 shows the T_C (onset) decreased monotonically with decreasing oxygen content in the $LnBa_2Cu_3O_{7-x}$ samples.

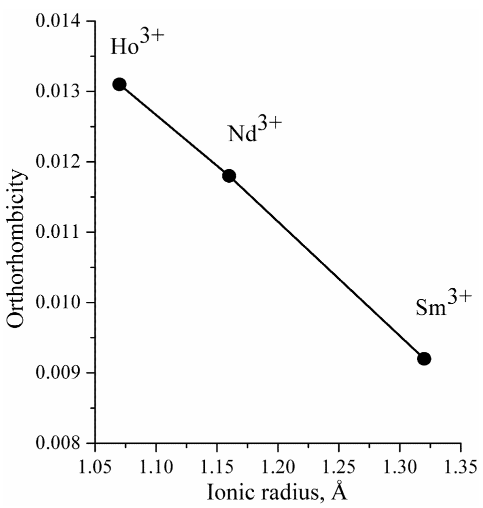

Fig. 5. Correlation between orthorhombicity and ionic radius.

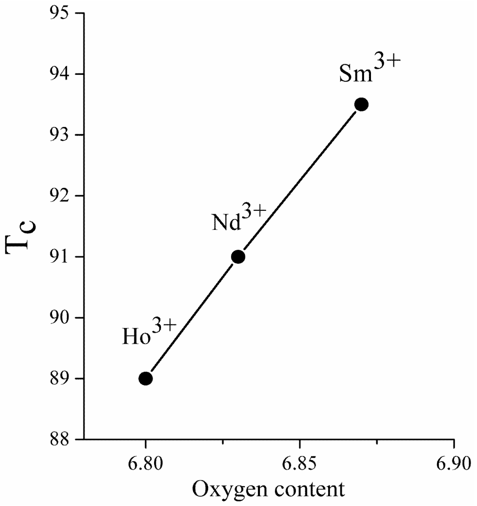

Fig. 6. T_C *vs.* oxygen content for $LnBa_2Cu_3O_{7-x}$ superconducting cuprates.

Similarly, Fig. 7 shows that the correlation between T_C (onset) and the hole concentration in the Cu–O chains had the same trend. T_C (onset) increased from 89 to 93.5 K on increasing n_h from 0.315 to 0.375.

Hence, it can be concluded that the hole carrier density in the sol–gel derived $LnBa_2Cu_3O_{7-x}$ samples corresponded to their optimal values.[19,20] Thus, these results indicate that no underdoping or overdoping effects can be observed in the Ln-123 phases.

The relationship between T_C (onset) and orthorhombicity is plotted in Fig. 8, from which it can be seen T_C decreased with increasing orthorhombicity.

The decrease in T_C with increasing orthorhombicity could be related to electronic transfer from the Cu–O linear chains to the CuO_2 planes.[9,21,22] Therefore, from the obtained results, it can be concluded that in the series of Sm-, Nd- and Ho-substituted Ln-123 samples, the occupancy of the oxygen atom sites at O(4) relatively decreases. On the contrary, the occupancy of oxygen atom at O(5) increased in the range from Sm^{3+} to Ho^{3+}. Only in this case, does the relative difference between the *b* and *a* parameters decrease, resulting in a decrease in the orthorhombicity.

Finally, the T_C (onset) correlated very well with the values of the ionic radius of the lanthanide ions (Fig. 9).

As can be seen from Fig. 9, the T_C value increased linearly with increasing ionic radius, probably indicating the highest hole concentration to be in the $SmBa_2Cu_3O_{7-x}$ sample.

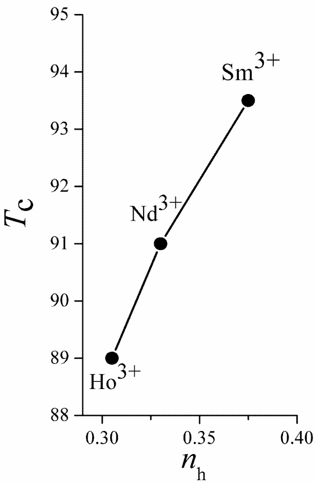

Fig. 7. T_C *vs.* hole concentration for $LnBa_2Cu_3O_{7-x}$ superconducting cuprates.

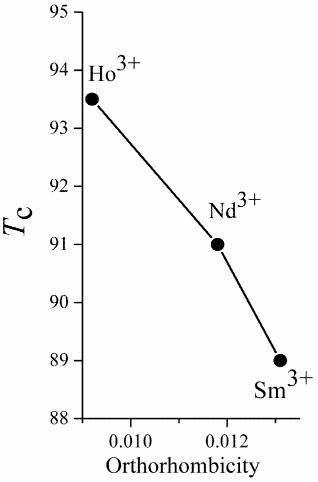

Fig. 8. T_C *vs.* orthorhombicity for $LnBa_2Cu_3O_{7-x}$ superconducting cuprates.

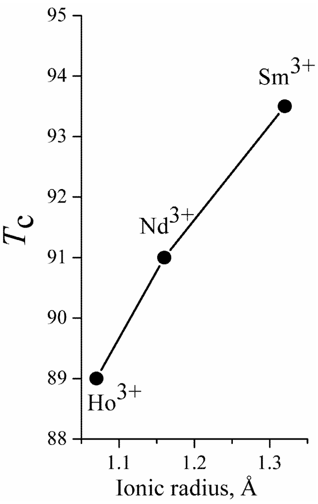

Fig. 9. T_C *vs.* ionic radius of the lanthanide ion for $LnBa_2Cu_3O_{7-x}$ superconducting cuprates.

CONCLUSIONS

The present study demonstrated the versatility of the sol–gel method to yield superconducting $LnBa_2Cu_3O_{7-x}$ (Ln-123) samples. The correlation between the T_C values for different lanthanides (Ln–Ho, Nd and Sm) in the Ln-123 compound and different parameters, such oxygen stoichiometry, hole concentration, orthorhombicity and ionic radius, were investigated. The T_C values of the $LnBa_2Cu_3O_{7-x}$ oxides increased progressively with increasing oxygen content, hole concentration and ionic radius of the lanthanide ion. However, the T_C decreased with increasing orthorhombicity of the Ln-123 phase.

ИЗВОД

СИНТЕЗА И КАРАКТЕРИЗАЦИЈА Ln–123 СУПЕРПРОВОДНИКА

ARTURAS ZALGA[1], REMIGIJUS JUSKENAS[2], ALGIRDAS SELSKIS[2],
DARIUS JASAITIS[1] и AIVARAS KAREIVA[1]

[1]*Faculty of Chemistry, Vilnius University, Naugarduko 24, LT-03225 Vilnius* и
[2]*Institute of Chemistry, A. Gostauto 9, LT-01108 Vilnius, Lithuania*

Сол–гел метода је примењена за припрему полазних једињења при добијању $NdBa_2Cu_3O_{7-x}$ (Nd-123) и $SmBa_2Cu_3O_{7-x}$ (Sm-123) суперпроводних једињења. Синтеровани производи испитивани су анализом дифракције X-зрака (XRD) скенирајућом електронском микроскопијом (SEM). У праховима који су синтеровани на 950 и 1000 °C формирани су монофазни Nd-123 и Sm-123 суперпроводници. Међутим, формирање Nd-123 и Sm-123 фаза из полазних једињења добијених сол–гел поступком на вишим температурама (1050 и 1100 °C) није се одиграло због процеса топљења. Такође је процењен и однос између T_C различитих лантанида (Ln–Ho, Nd и Sm) у једињењу Ln-123 и степена орторомбичности, односно стехиометрије кисеоника.

(Примљено 10. јануара, ревидирано 12. новембра 2007)

REFERENCES

1. O. F. Schilling, *Supercond. Sci. Technol.* **17** (2004) L17
2. L. C. Pathak, S. K. Mishra, *Supercond. Sci. Technol.* **18** (2005) R67
3. J. G. Noudem, E. S. Reddy, M. Tarka, M. Noe, G. J. Schmitz, *Supercond. Sci. Technol.* **14** (2001) 363
4. K. Iida, J. Yoshioka, N. Sakai, M. Murakami, *Physica C* **370** (2002) 53
5. M. Andersson, O. Rapp, Z. Hegedus, T. L. Wen, M. Nygren, *Physica C* **190** (1992) 255
6. R. Nagarajan, C. N. R. Rao, *J. Mater. Chem.* **3** (1993) 969
7. K. Ogasawara, N. Sakai, M. Murakami, *J. Cryst. Growth* **229** (2001) 358
8. E. S. Reddy, G. J. Schmitz, *Supercond. Sci. Technol.* **15** (2002) 727
9. C. H. Chin, H.-C. I. Kao, C. M. Wang, *Mater. Chem. Phys.* **89** (2005)143
10. A. Zalga, E. Matulionis, D. Jasaitis, R. Juskenas, A. Selskis, A. Kareiva, *Env. Chem. Phys.* **25** (2003) 43
11. M. Karppinen, L. Niinisto, H. Yamauchi, *J. Therm. Anal.* **48** (1997) 1123
12. P. Benzi, E. Bottizzo, N. Rizzi, *J. Cryst. Growth* **269** (2004) 625
13. A. N. Christensen, *Acta Chem. Scand.* **46** (1992) 909
14. J. Linden, M. Lippmaa, J. Miettinen, I. Tittonen, T. Katila, A. Kareiva, M. Karppinen, L. Niinistö, J. Valo, M. Leskelä, *Phys. Rev. B* **50** (1994) 4154
15. L. Vilciauskas, A. Beganskiene, A. Kareiva, K. Gibson, P. Ziegler, H.-J. Meyer, *J. Mater. Sci. Lett.* **41** (2006) 579
16. D. C. Harris, T. A. Hewston, *J. Solid State Chem.* **69** (1987) 182
17. P. Lanza, G. Rossi, *Anal. Chim. Acta* **244** (1991) 253
18. A. Kareiva, S. Tautkus, *Chemija* **4** (1997) 58
19. G. Nenartaviciene, A. Beganskiene, S. Tautkus, D. Jasaitis, A. Kareiva, *Chem. Phys.* **332** (2007) 225
20. A. Biju, R. P. Aloysius, U. Syamaprasad, *Mater. Lett.* **61** (2006) 648
21. X. S. Wu, J. Gao, *Physica C* **313** (1999) 79
22. Y. Yasukawa, T. Nakane, M. Karppinen, H. Yamauchi, *Physica C* **357**–**360** (2001) 230.